Pressure dependence of superconductivity in simple cubic phosphorus

Kevin T. Chan, Brad D. Malone, and Marvin L. Cohen
Department of Physics, University of California, Berkeley, California 94720, USA
and Materials Sciences Division, Lawrence Berkeley National Laboratory, Berkeley, California 94720, USA
(Received 26 April 2013; revised manuscript received 5 July 2013; published 30 August 2013)

The electronic structure and lattice dynamics for simple cubic (sc) P are calculated over the pressure range 0–70 GPa from first principles using the local-density approximation. The R phonon mode is found to be unstable below 20 GPa in the harmonic approximation, but may be stable down to a pressure less than 20 GPa when anharmonicity is considered. The electron-phonon coupling is calculated for pressures above 20 GPa, and the superconducting transition temperature T_c is found to decrease with increasing pressure throughout this pressure range. The result is in agreement with experimental results above 30 GPa. In contrast to experiment, no evidence for a decrease in T_c with decreasing pressure below 30 GPa is found. The structural transition from rhombohedral $A7$ to sc is also investigated. An interesting two-step transition is found to occur theoretically which may have relevance for the pressure dependence of T_c. Possible explanations for the discrepancy with experiment are discussed.

DOI: 10.1103/PhysRevB.88.064517 PACS number(s): 74.62.Fj, 74.70.Ad, 74.25.Kc, 74.20.Pq

I. INTRODUCTION

One hundred years after its discovery,[1] superconductivity remains one of the most exciting subjects in condensed-matter physics. In addition to the recent discoveries of unconventional superconductivity in the iron-based superconductors,[2,3] there have been a large number of interesting developments in the superconductivity of simpler materials, including MgB_2,[4,5] diamond,[6] cubic silicon doped with boron,[7] and the surprising large superconducting transition temperature (T_c) of 20 K for lithium under pressure.[8]

A large number of other elemental solids have been found to be superconducting, many in the past 20–30 years with the aid of much-improved diamond-anvil cells.[9] The experimental ability to vary the pressure over several hundred GPa has allowed for superconductivity to be explored in high-pressure polytypes not accessible at lower pressures, as well as the study of the pressure dependence of T_c within single phases which can vary because of underlying electronic and vibrational changes that occur as a material is compressed.

Phosphorus is semiconducting and takes on the orthorhombic $A17$ structure at ambient pressure and temperature.[10,11] Under the application of pressure it transforms into the semimetallic $A7$ structure at 4.5 GPa and to the metallic simple cubic (sc) phase at 10 GPa,[10,11] which is the stable form of phosphorus up to a pressure of 107 GPa.[12] Reports of superconductivity in the sc phase are now over 40 years old.[13,14] However, the maximal value and pressure dependence of T_c remain the subject of much controversy in the literature. Part of the confusion stems from the fact that the nature of the pressure variation of T_c depends strongly on the path taken in the P-T diagram.[15,16] While some differences can likely be attributed to incomplete phase transformations along particular paths, there is still discrepancy in the experimental results for the pressure dependence of samples that are believed to be fully transformed to the sc structure. Some experimental results indicate that T_c of the sc phase should be approximately 6 K and vary only weakly on pressure.[16] Others report that T_c should exhibit a two-peak structure with the largest peak occurring near 23 GPa with a transition temperature of $\sim$10 K.[17] The most recent results show only a single peak around 32 GPa with a maximal T_c of 9.5 K.[18]

Unfortunately, the previous theoretical results have not been able to resolve this discrepancy. Early estimates[19] of the pressure variation of T_c show a single peaked structure with the peak position near the second peak of the experimental results of Ref. 17. These calculations rely on approximations to the average phonon frequency entering into the McMillan equation for T_c and do not take into account the variation of the phonon spectrum with pressure. Other estimates establish that the electron-phonon (e-p) coupling strength is large enough to roughly account for the range of the experimentally observed T_c, but, lacking a detailed description of the phonon spectra, are unable to reliably establish the trend with increasing pressure.[20] A more recent calculation predicts that T_c should instead be relatively constant over the full range of stability of the sc phase;[21] this pressure variation is similar to the experimental results reported in Ref. 16. These calculations, which do not predict a drop in T_c at high pressures, are in stark disagreement with the most recent experimental results taken at high pressure in Ref. 18. Another theoretical study[22] found a calculated T_c that rose slightly from about 8.5 to 11 K as the pressure increased from 10 to 35 GPa. This study considered the change in phonon frequencies with pressure, but only estimated the Debye temperature from the calculated bulk modulus.

In the present study we hope to shed light on the pressure dependence of the transition temperature in simple cubic phosphorus. Towards this aim, we have performed fully *ab initio* calculations of the e-p coupling strength as a function of pressure over a wide range of the stability of the sc phase. In contrast to previous calculations, we calculate the lattice dynamics at each pressure from first principles. We find that at higher pressures, T_c decreases with increasing pressure, in good agreement with some experiments. However, we find no evidence of the decrease in T_c as pressure is decreased at lower pressures. Our harmonic phonon calculations indicate that the sc structure has an instability in the R phonon mode at a pressure higher than observed in experiment. We therefore calculate anharmonic phonon frequencies for the R mode,

and find that the phonon modes are stable down to 5 GPa. We also investigate the $A7$ to sc transition in P and find an interesting two-step transition that may have implications for the superconducting T_c.

II. METHODS

The e-p coupling formalism followed in the present study is the same as in Ref. 23. For convenience, we reproduce the relevant formulas here. The e-p matrix element for the scattering of an electron in band n at wave vector $\mathbf{k}$ to a state in band m with wave vector $\mathbf{k}+\mathbf{q}$ by a phonon with mode index ν at wave vector $\mathbf{q}$ is

$$g^{\nu}_{mn}(\mathbf{k},\mathbf{q}) = \left(\frac{\hbar}{2M\omega_{\mathbf{q}\nu}}\right)^{1/2} \langle m,\mathbf{k}+\mathbf{q}|\delta_{\mathbf{q}\nu}V_{\mathrm{SCF}}|n,\mathbf{k}\rangle. \quad (1)$$

In this expression, $|n,\mathbf{k}\rangle$ is the bare electronic Bloch state, $\omega_{\mathbf{q}\nu}$ is the screened phonon frequency, M is the ionic mass, and $\delta_{\mathbf{q}\nu}V_{\mathrm{SCF}}$ is the derivative of the self-consistent potential with respect to a collective ionic displacement corresponding to phonon wave vector $\mathbf{q}$ and mode ν.

The phonon linewidth is given by

$$\gamma_{\mathbf{q}\nu} = \pi\omega_{\mathbf{q}\nu}\sum_{mn}\sum_{\mathbf{k}} w_{\mathbf{k}}\left|g^{\nu}_{mn}(\mathbf{k},\mathbf{q})\right|^2\delta(\epsilon_{m,\mathbf{k}+\mathbf{q}}-\epsilon_F) \times \delta(\epsilon_{n,\mathbf{k}}-\epsilon_F), \quad (2)$$

where $w_{\mathbf{k}}$ is the k-point weight (normalized such that $\sum_{\mathbf{k}} w_{\mathbf{k}} = 2$), $\epsilon_{n,\mathbf{k}}$ is the energy of the bare electronic Bloch state, and ϵ_F is the Fermi energy.

The sum over electron wave vectors $\mathbf{k}$ is performed on a uniform grid over the whole Brillouin zone (BZ).

The phonon-mode-dependent coupling constant is given by

$$\lambda_{\mathbf{q}\nu} = \frac{\gamma_{\mathbf{q}\nu}}{\pi N(\epsilon_F)\omega^2_{\mathbf{q}\nu}}. \quad (3)$$

In terms of the phonon linewidths, the Eliashberg spectral function $\alpha^2F(\omega)$ can be written as[24]

$$\alpha^2F(\omega) = \frac{1}{2\pi N(\epsilon_F)}\sum_{\mathbf{q}\nu} w_{\mathbf{q}}\frac{\gamma_{\mathbf{q}\nu}}{\omega_{\mathbf{q}\nu}}\delta(\omega-\omega_{\mathbf{q}\nu}). \quad (4)$$

The sum over phonon wave vector $\mathbf{q}$ is performed on a uniform grid over the irreducible BZ, with appropriate weights $w_{\mathbf{q}}$, where $\sum_{\mathbf{q}} w_{\mathbf{q}} = 1$. In Eqs. (3) and (4), $N(\epsilon_F)$ is the density of states at ϵ_F per unit cell and per spin. The coupling constant λ is given by the integral

$$\lambda = 2\int_0^{\infty}\frac{\alpha^2F(\omega)}{\omega}d\omega. \quad (5)$$

Other important frequency moments of $\alpha^2F(\omega)$ are defined as follows:

$$\langle\omega^2\rangle = \frac{2}{\lambda}\int_0^{\infty}\omega\alpha^2F(\omega)d\omega \quad (6)$$

and

$$\omega_{\ln} = \exp\left(\frac{2}{\lambda}\int_0^{\infty}\ln\omega\frac{\alpha^2F(\omega)}{\omega}d\omega\right). \quad (7)$$

We determine T_c using the Allen-Dynes-modified McMillan equation:[25,26]

$$T_c = \frac{\omega_{\ln}}{1.2}\exp\left(-\frac{1.04(1+\lambda)}{\lambda-\mu^*(1+0.62\lambda)}\right), \quad (8)$$

where μ^* is the Coulomb pseudopotential.[27]

First-principles electronic structure calculations are performed with the QUANTUM-ESPRESSO code (QE)[28] within density-functional theory[29,30] using the plane-wave pseudopotential method[31,32] along with the local-density approximation (LDA)[33,34] to the exchange-correlation energy. A norm-conserving pseudopotential was constructed for P using the Troullier-Martins scheme[35] as implemented in the APE code.[36] The outermost $3s^23p^3$ electrons are treated as valence electrons and a nonlinear-core correction (NLCC) has been added.[37] A plane-wave cutoff of 60 Ry for the valence wave functions is used. Self-consistent charge density and total-energy calculations for sc P are performed using a $30\times30\times30$ Monkhorst-Pack[38] (MP) k grid with 0.03 Ry Marzari-Vanderbilt (MV) smearing[39] for the occupations of the electronic states. The sc lattice constant at a given pressure is determined by relaxing the lattice constant until the calculated pressure is within 0.05 GPa of the target pressure.

Electron-phonon calculations are performed for the sc structure between 20 and 70 GPa. In order to converge the e-p quantities while maintaining a reasonable computational cost, we use the electron-phonon Wannier (EPW) method,[40] as implemented in the EPW code,[41] to interpolate e-p matrix elements calculated on coarse electron and phonon grids to fine k and q grids. Maximally localized Wannier functions[42,43] for use in the EPW method are generated using the WANNIER90 code.[44]

Bloch functions on an $8\times8\times8$ k grid in the BZ are used to generate Wannier functions for the lowest nine bands. Phonons in the harmonic approximation are calculated on an $8\times8\times8$ q grid in the BZ using density functional perturbation theory[45] as implemented in QE.

Matrix elements are interpolated onto a $100\times100\times100$ Γ-centered k grid for the phonon linewidth calculations; the δ functions of Eq. (2) are approximated by Gaussians of width 0.02 Ry. A $30\times30\times30$ Γ-centered fine q grid with a δ-function smearing of 2 meV is used for the calculation of $\alpha^2F(\omega)$ [Eq. (4)]. With the chosen computational parameters, λ is estimated to be converged to less than 0.01.

In addition to e-p calculations in the harmonic approximation, we also estimate anharmonic phonon frequencies for the sc R mode. With the frozen phonon method, the anharmonic phonon modes can be determined by considering atomic displacements with wave vector R, and solving the Schrödinger equation in a potential given by the total energy versus atomic displacement in three dimensions. Such a solution for a general three-dimensional potential is difficult, so we estimate the phonon modes by fixing the phonon polarization along a given direction and considering the one-dimensional potential. We determine the phonon frequency as the difference in energies of the ground and first excited states in the one-dimensional potential. We consider polarizations in the [111] and [100] directions.

The $A7$ to sc structural transition in P is studied using variable-cell relaxation calculations; the method is similar to that used in Ref. 23. Target pressures between 0 and 25 GPa are considered. A $30 \times 30 \times 30$ MP k grid in the rhombohedral BZ with 0.03 Ry MV smearing is used. Initial values of $\cos\alpha = 0.536$ and $u = 0.223$, taken from experiment at 6.7 GPa,[11] are used for the starting structure for the relaxations. Structures are relaxed until components of the forces on the atoms are less than 10^{-4} Ry/a.u. and the pressure is within 0.05 GPa of the target pressure.

III. RESULTS

A. Electronic structure, phonons, and electron-phonon coupling for sc P

The calculated volume and lattice constant as a function of pressure are given in Table I. The calculated total energy versus volume data are fit to a Birch-Murnaghan equation of state (EOS),[46] giving $V_0 = 14.04$ Å^3, $B_0 = 131.6$ GPa, and $B_0' = 3.92$ for the equilibrium volume, bulk modulus, and the pressure derivative of the bulk modulus, respectively. The equilibrium volume is somewhat smaller than that found from fitting a Murnaghan or Birch-Murnaghan EOS to experimental data (15.2 Å^3 for Ref. 11 and 15.52 Å^3 for Ref. 12), and the calculated B_0 somewhat larger than experiment (95 GPa for Ref. 11 and 70.7 GPa for Ref. 12); our results are consistent with the tendency of the LDA to overbind. Our EOS parameters are in good agreement with recent previous first-principles calculations.[22,47–49] Table I also shows, for each calculated volume, the corresponding experimental pressure, P_{expt1} or P_{expt2}, obtained from the Murnaghan or Birch-Murnaghan EOS with parameters from Ref. 11 or 12, respectively. For example, a Murnaghan EOS with equilibrium volume parameter $V_0 = 15.2$ Å^3 and bulk modulus parameter $B_0 = 95$ GPa from Ref. 11 gives a pressure $P_{\text{expt1}} = 8.0$ GPa for a volume $V = 14.06$ Å^3.

A previous calculation[22] indicates that the generalized-gradient approximation (GGA) gives an equilibrium volume and bulk modulus that is in better agreement with experimental results than the LDA for sc P, though not dramatically so.

TABLE I. Calculated pressure P_{calc}, volume V, lattice constant a, and corresponding experimental pressures P_{expt1} and P_{expt2} for sc P. The pressures P_{expt1} and P_{expt2} are determined from the volume by using the equation-of-state parameters given in Refs. 11 and 12, respectively.

P_{calc} (GPa)	V (Å^3)	a (Å)	P_{expt1} (GPa)	P_{expt2} (GPa)
0	14.06	2.414	8.0	8.9
5	13.55	2.384	12.3	13.5
10	13.13	2.359	16.3	18.1
15	12.77	2.337	20.0	22.7
20	12.45	2.318	23.6	27.3
25	12.16	2.300	27.0	32.1
30	11.91	2.283	30.3	36.9
40	11.45	2.254	36.8	46.8
50	11.06	2.228	42.9	57.0
60	10.73	2.206	48.7	67.3
70	10.44	2.185	54.4	77.9

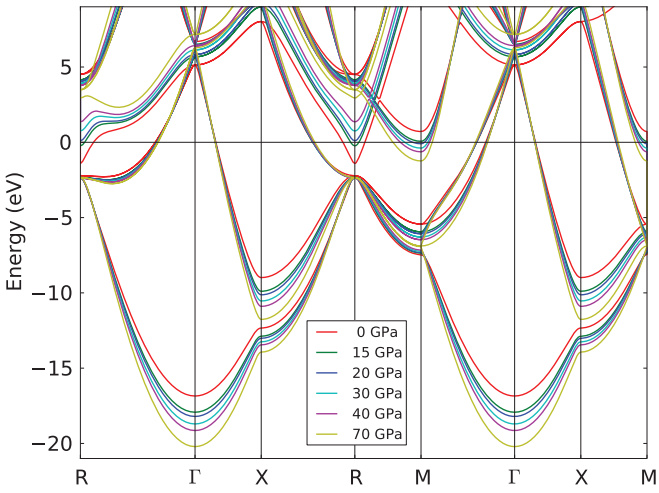

FIG. 1. (Color online) Band structure of the simple cubic phase of P for a number of pressures. The Fermi level is located at zero energy.

In the present work, we restrict ourselves to the LDA so as to facilitate comparison with previous calculations of superconductivity that use the LDA[19,20,22] and because the LDA has been used successfully to study superconductivity in other simple materials under pressure.[23,50–53] Calculations of superconductivity in sc P using the GGA could be interesting but are beyond the scope of the present work.

The band structure of sc P as a function of pressure is shown in Fig. 1. The largest changes near ϵ_F as a function of pressure happen around the points R and M in the Brillouin zone. The valence band at R, occupied for pressures below 15 GPa, rises in energy as the structure is compressed and becomes unoccupied before a pressure of 20 GPa. The behavior at the M point is the reverse, dropping lower in energy with increasing pressure. This behavior is in agreement with that found in previous calculations,[19,20,22,47] although the precise occupations of these specific bands at a given pressure differ slightly between calculations. At 0 GPa, $N(\epsilon_F)$ is 0.309 states/eV atom (for both spins); it decreases slightly when pressure increases to 20 GPa, then increases and levels off at higher pressures (Table II). This general trend also agrees with previous calculations.[19,22] Bands 2 and 3 do not change dramatically with pressure near ϵ_F.

TABLE II. Calculated frequency moments, $N(\epsilon_F)$, $\langle g^2\rangle$, λ, and T_c for sc P at various pressures. Equation (12) in the text is used to determine the Coulomb pseudopotential μ^* as a function of pressure in the calculation of T_c, with $\mu^* = 0.18$ at $P_{\text{calc}} = 25$ GPa.

P_{calc} (GPa)	$\omega_{\ln}$ (K)	$\langle\omega^2\rangle^{1/2}$ (K)	$N(\epsilon_F)$ (states/eV atom)	$\langle g^2\rangle$ (eV/Å)^2	λ	T_c (K)
20	418	449	0.292	60.61	0.795	10.26
25	435	468	0.296	63.05	0.776	9.64
30	444	482	0.301	65.32	0.771	9.39
40	456	506	0.303	68.81	0.739	8.24
50	464	527	0.305	71.60	0.714	7.26
60	469	546	0.306	74.13	0.693	6.43
70	469	561	0.306	76.34	0.676	5.77

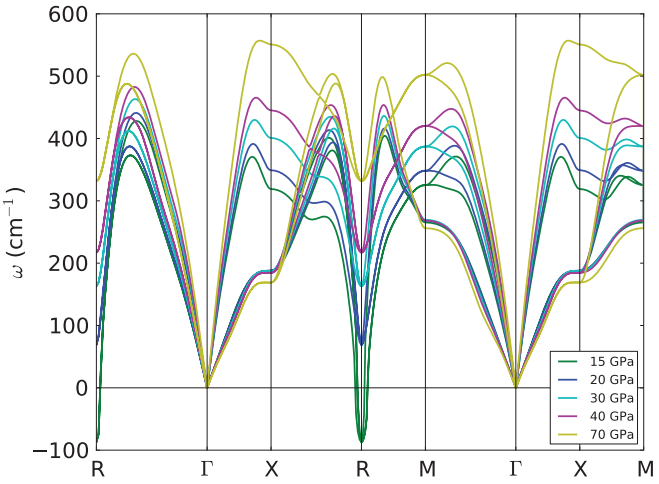

FIG. 2. (Color online) Phonon dispersion for P in the simple cubic phase for a number of pressures. The dynamical instability at the R point at lower pressures corresponding to the distortion towards the rhombohedral $A7$ structure can be seen.

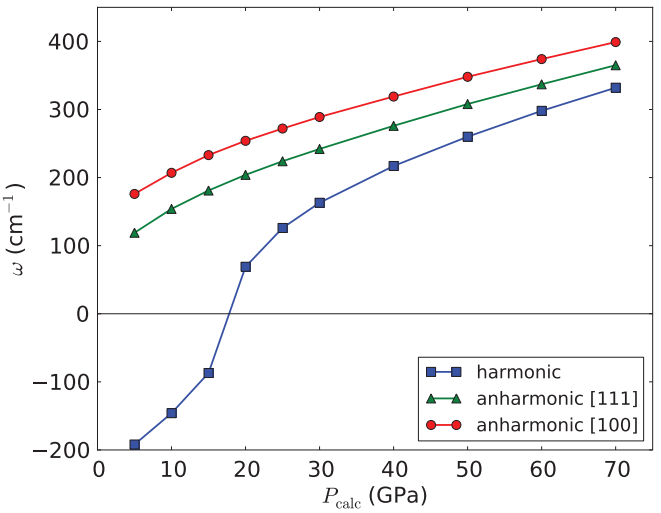

FIG. 3. (Color online) Phonon frequencies for R phonon mode as a function of pressure. The anharmonic frequencies are estimated for polarizations along the [111] and [100] directions.

The phonon dispersions are plotted in Fig. 2 for several pressures. The majority of the phonon frequencies are found to harden with increasing pressure. An exception is the transverse branch which shows a slight softening with increasing pressure along the ΓX, ΓM, and XM directions. This softening agrees with previous calculations and is consistent with an instability of the sc structure at pressures higher than those calculated in the present study.[54] The overall hardening of phonon modes can also be seen in the phonon density of states $F(\omega)$, shown in Fig. 4 (top).

Below 20 GPa the lattice distortion corresponding to the wave vector R is found to have imaginary frequency, suggesting that below 20 GPa, P is not stable in the sc structure and instead takes on the rhombohedral $A7$ structure. This result differs from experiment,[11] where the sc structure is stable down to about 10 GPa (corresponding to a pressure of less than 5 GPa in our calculations; see Table I). However, previous calculations for As in the sc structure show that the R phonon mode is anharmonic near the transition to the $A7$ structure.[55] We therefore estimate the anharmonic phonon frequencies for the R mode to determine if, theoretically, the sc structure might be stable at these lower pressures. The results for polarization in the [100] and [111] directions are given in Fig. 3 for various pressures.

At large pressures, anharmonic corrections are small. As the pressure decreases, the anharmonicity of the R mode increases. The anharmonic phonon frequencies are real down to a theoretical pressure of 5 GPa and the R mode does not go completely soft. Therefore, the sc structure may remain stable to pressures lower than what is suggested by considering only the harmonic approximation. The transition to the $A7$ structure is considered further in Sec. III B.

We now present results for e-p coupling in sc P. We restrict ourselves to the harmonic approximation, and therefore only consider pressures from 20 to 70 GPa. The Eliashberg spectral function $\alpha^2F(\omega)$ is shown in Fig. 4 (bottom) for several pressures. The shape of $\alpha^2F(\omega)$ is very similar to that of $F(\omega)$, with somewhat enhanced weight at very low frequencies and high frequencies, as compared to midrange frequencies. The shift of $\alpha^2F(\omega)$ to higher frequencies as pressure is increased follows the trend for $F(\omega)$ and leads to lower integrated λ values. In the spectral function for 70 GPa one can observe the larger coupling at low phonon energies relative to the curves for lower pressures. This enhanced coupling is related to the softening of the transverse modes that is seen in the phonon dispersion in Fig. 2.

The wave-vector-resolved e-p couplings $\lambda_{\mathbf{q}} = \sum_\nu \lambda_{\mathbf{q}\nu}$ allow us to examine which modes contribute most strongly to the overall e-p coupling. Figure 5 shows $\lambda_{\mathbf{q}}$ (top) and the nesting function $\xi_{\mathbf{q}}$ (bottom) along several high-symmetry lines in the BZ for several pressures. The nesting function is defined as

$$\xi_{\mathbf{q}} = \sum_{mn} \sum_{\mathbf{k}} w_{\mathbf{k}} \delta(\epsilon_{m,\mathbf{k}+\mathbf{q}} - \epsilon_F)\delta(\epsilon_{n,\mathbf{k}} - \epsilon_F) \qquad (9)$$

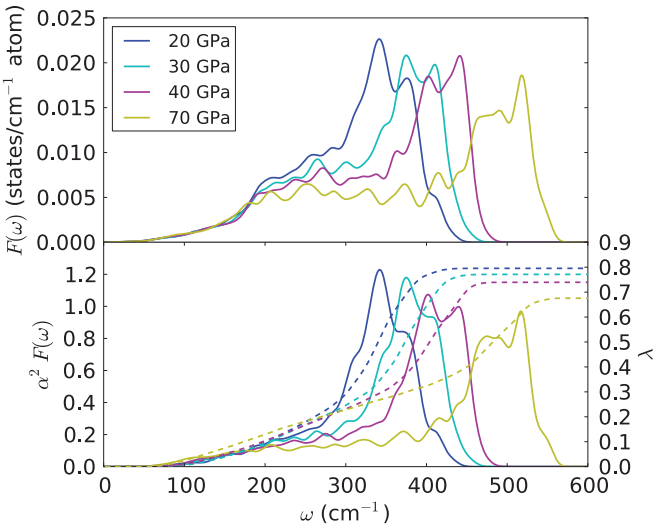

FIG. 4. (Color online) Phonon density of states $F(\omega)$ (top), Eliashberg spectral function $\alpha^2F(\omega)$ (bottom, solid), and integrated λ (bottom, dashed) for sc P for a number of pressures.

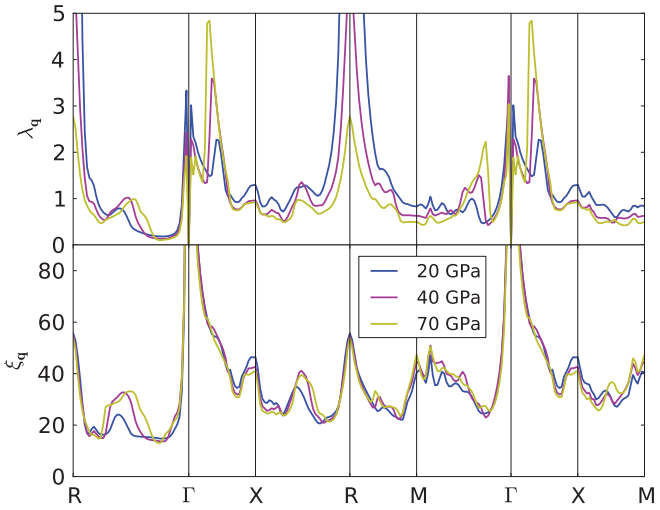

FIG. 5. (Color online) Electron-phonon coupling constant $\lambda_{\mathbf{q}}$ (top) and nesting function $\xi_{\mathbf{q}}$ (bottom) along high-symmetry lines in the Brillouin zone for sc P at various pressures. Values for $\lambda_{\mathbf{q}}$ at R are 57, 6.0, and 2.8 for 20, 40, and 70 GPa, respectively.

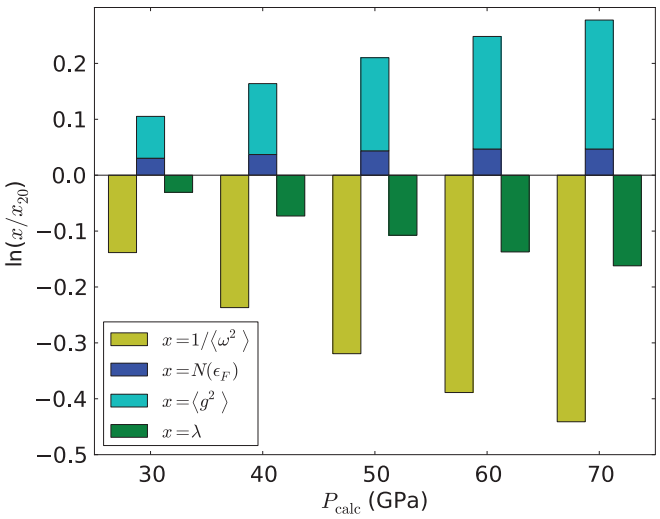

FIG. 6. (Color online) Trends in average phonon frequency $\langle\omega^2\rangle$, $N(\epsilon_F)$, average e-p matrix element $\langle g^2\rangle$, and e-p coupling λ as a function of pressure. The subscript "20" denotes the value at 20 GPa.

[compare to Eq. (2)] and describes the phase space for scattering across the Fermi surface. It can be seen that the coupling at the softened mode R is very strong, but that there are also other strongly coupled regions throughout the Brillouin zone. The large coupling at R and X can partially be explained by large Fermi-surface nesting at these wave vectors. Wave vectors approximately midway between R and Γ and between X and R show large coupling and large nesting as well. Interestingly, peaks in $\lambda_{\mathbf{q}}$ can be seen at specific wave vectors between Γ and X and M and Γ that increase with pressure, contrary to the overall trend in $\lambda_{\mathbf{q}}$. Little or no corresponding enhancement of $\xi_{\mathbf{q}}$ can be seen at these wave vectors. However, these peaks correspond to wave vectors at which phonon softening occurs at 70 GPa (Fig. 2) and are related to the aforementioned instability of the sc structure at higher pressures. These phonon modes contribute to the slightly enhanced coupling around 100 cm^{-1} seen in the $\alpha^2F(\omega)$.

Frequency moments of $\alpha^2F(\omega)$ and the total e-p coupling parameter λ, along with $N(\epsilon_F)$, are given in Table II for the pressures calculated in this work. To facilitate comparison with previous studies, we also include values for $\langle g^2\rangle$, the average over the Fermi surface of the squared e-p matrix elements [note that $\langle g^2\rangle$ does not include the factor $(\hbar/2M\omega_{\mathbf{q}\nu})^{1/2}$ present in Eq. (1)]. These quantities are related by[25]

$$\lambda = \frac{N(\epsilon_F)\langle g^2\rangle}{M\langle\omega^2\rangle}. \tag{10}$$

In Eq. (10), $N(\epsilon_F)$ is for a single spin (i.e., one-half of the value given in Table II, which is for both spins). Taking the natural logarithm of the quantities in Eq. (10) and normalizing to their values at 20 GPa, we have

$$\ln\frac{\lambda}{\lambda_{20}} = \ln\frac{N(\epsilon_F)}{N(\epsilon_F)_{20}} + \ln\frac{\langle g^2\rangle}{\langle g^2\rangle_{20}} + \ln\frac{\langle\omega^2\rangle_{20}}{\langle\omega^2\rangle}, \tag{11}$$

where the subscript 20 denotes the value at 20 GPa. The results as a function of pressure are plotted in Fig. 6.

We find that the contribution of $N(\epsilon_F)$ to λ increases slightly from 20 to 30 GPa, and then remains almost constant as pressure increases. The contribution from the matrix elements does increase significantly with pressure. However, the contribution from increasing phonon frequencies is larger and results in a net decrease in λ as pressure increases.

The magnitude and pressure trend of $N(\epsilon_F)$ agrees well with previous studies.[19,20,22] The increase in average phonon frequency with increasing pressure is also in agreement with previous studies that consider this pressure trend.[20,22] However, our average phonon frequencies are significantly larger in magnitude for similar pressures (~450–500 K for our calculations versus ~350–400 K for other works). We believe our calculations to be more accurate, since we have calculated the full phonon dispersion from first principles, while previous studies used estimates. Likewise, the trends in $\langle g^2\rangle$ with pressure agree with previous studies, but the magnitude of our values are roughly twice as large as those in other works. The origin of this difference is unclear, but may be related to the difference in calculational methods; previous studies used augmented plane-wave or muffin-tin orbital methods. Thus, the rough agreement in magnitude of λ between the present study and previous studies is somewhat fortuitous.

Table II also shows T_c calculated using the McMillan equation [Eq. (8)]. The Coulomb pseudopotential parameter μ^* is determined by using a modified Bennemann-Garland relation[56–58] which relates μ^* to $N(\epsilon_F)$:

$$\mu^* = \frac{CN(\epsilon_F)}{1 + N(\epsilon_F)}. \tag{12}$$

Since $N(\epsilon_F)$ varies little with pressure, μ^* is almost constant. The constant C is obtained by matching the calculated T_c to that of experiment at one pressure. We use the experimental results for T_c of Karuzawa *et al.*[18] because they extend to higher pressures than other studies.

Because, for a given pressure, the volume calculated using the LDA differs from that of experiment, we have chosen

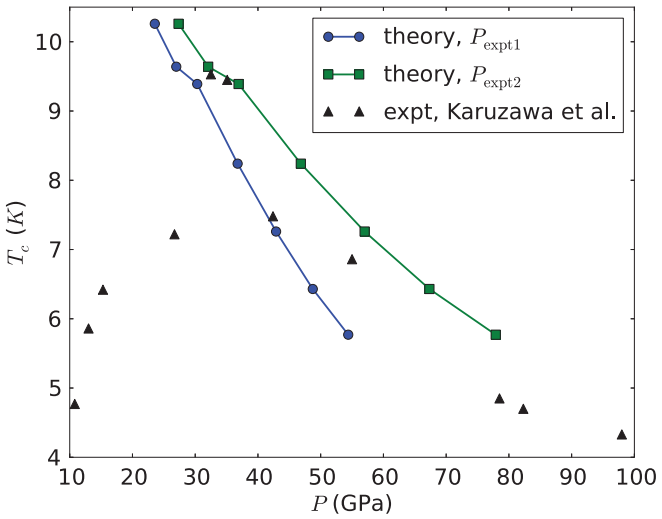

FIG. 7. (Color online) Calculated T_c as a function of pressure compared to the experimental results of Karuzawa *et al*. (Ref. 18). For the calculations, pressures are shifted to match experiment, according to Table I.

to shift the calculated pressure P_{calc} to an "experimental" pressure P_{expt1} or P_{expt2} (as given in Table I and described in Sec. III A), for the purposes of comparison. This procedure is equivalent to comparing theory and experiment at the same *volume*. While this procedure is not rigorously justified, it gave good agreement between experiment and theory for As under pressure.[23] A similar shift was used in studying superconductivity in Al and Li under pressure.[51] We note that if this procedure for shifting the pressure is not used, there are only small quantitative differences in the results.

With this pressure shift, we find that setting μ^* to 0.18 for $P_{\text{calc}} = 25$ GPa allows us to match our results to the experimental maximum T_c at around 32 GPa; hence $C = 0.79$ in Eq. (12).

A μ^* of 0.18 is somewhat larger than the generally accepted value ($\sim$0.13) for conventional superconductors.[25] Some studies indicate that such a large μ^* is applicable for Li,[51,53,59] so it is possible that the same is true for P. Alternatively, one could question whether it is valid to use the Eliashberg/McMillan formalism with the Coulomb pseudopotential or whether some alternate theory is required.

The calculated and experimental pressure dependence of T_c is shown in Fig. 7. The calculations showing a decrease in T_c with increasing pressure are in good agreement with the experimental data for pressures above 30 GPa (corresponding to $P_{\text{calc}} \approx$ 25–30 GPa). However, the calculated T_c continues to increase with decreasing pressure below 30 GPa; this result is in disagreement with the experimental data, which shows a drop in T_c at lower pressures.

The qualitative behavior of T_c(P) above 30 GPa can be understood by looking at Table II and Eq. (8). While $\omega_{\ln}$ increases with pressure, λ decreases with pressure, so the overall T_c decreases with pressure. For the calculations, these trends extend below 30 GPa. The disagreement between calculations and experiment raises questions about whether other physical effects are occurring in experiment that are not accounted for in the calculation.

B. *A*7 to sc transition

The stability of P in the sc structure below a theoretical pressure of 20 GPa was called into question by the soft R phonon mode calculated in the harmonic approximation. We therefore consider whether the $A7$ structure is more stable than the sc one in this pressure range. Similar theoretical studies of the $A7$ to sc transition in As have been performed.[23,60–63] Our calculated structural parameters for $A7$ P—the rhombohedral lattice constant a_{rhom}, rhombohedral angle α, and internal parameter u, as well as nearest-neighbor (d_1) and next-nearest-neighbor (d_2) distances—are given in Fig. 8. The relaxed structure is sc for pressures of 20 GPa and above, as indicated by $\alpha = 60^\circ$, $u = 0.25$, and $d_1 = d_2$. For pressures below 20 GPa, $u < 0.25$; this result is consistent with the imaginary frequency for the R mode found from the phonon calculations in the harmonic approximation. In this pressure range, we calculated the enthalpy for the sc phase and verified that it is higher than the enthalpy for the relaxed $A7$ phase, showing that the $A7$ phase is indeed favored.

Interestingly, the results indicate that there are two transitions that are well separated in pressure. Starting at low pressures in the $A7$ structure, in the first transition α becomes close to 60° between 0 and 5 GPa, while u increases only incrementally and is far from the cubic value of 0.25; α remains close to 60° above 5 GPa. In the second transition, u reaches 0.25 at a pressure between 15 and 20 GPa. The fact that a significant displacement u away from 0.25 induces only a small change in α for pressures between 5 and 15 GPa is surprising. By the symmetry of the sc structure, a displacement of the atoms with wave vector R must induce a rhombohedral distortion of the unit cell. Our results do not violate symmetry considerations, as $\alpha \neq 60^\circ$ below 20 GPa, but the fact that α is so close to 60° is unexpected.

In these calculations, the true $A7$ to sc transition occurs between 15 and 20 GPa (above 20 GPa when shifted to the corresponding experimental pressure), which is significantly higher than in experiment.[11] Possible reasons for this discrepancy are discussed in Sec. IV.

IV. DISCUSSION

A. Comparison of *e*-*p* coupling in P and As

It is interesting to compare the case of P to that of As. Like P, As has five valence electrons per atom and undergoes an $A7$ to sc structural transition as pressure is increased.[64,65] The experimentally measured T_c as a function of pressure for As (Ref. 55) has a peak structure similar to several experimental results for P.[17,18] The electronic and phononic structure for sc As[23] is similar to that of P; in particular, the Fermi surfaces for valence bands 2 and 3 (Fig. 1) have similar shapes.[20,47,66]

There are also important experimental differences between P and As. The $A7$ to sc transition pressure for P is around 10 GPa at room temperature, which is significantly lower than that for As, which has been measured to be 24–32 GPa.[64,65] The pressure at which As reaches a peak in superconducting T_c matches the pressure of the $A7$ to sc transition; this correspondence does not appear to be true for P. Furthermore, the maximum T_c for P ($\sim$10 K) is four times higher than that for As (2.4 K).

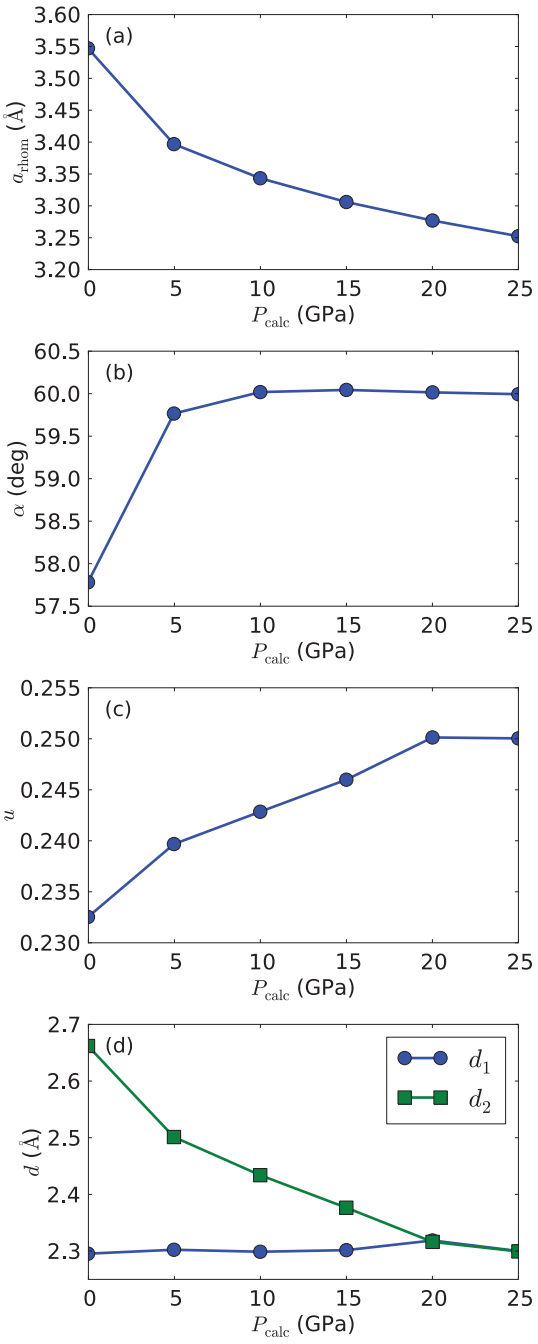

FIG. 8. (Color online) Lattice parameters (a) $a_{\rm rhom}$, (b) α, and (c) u, and (d) nearest-neighbor d_1 and next-nearest neighbor d_2 distances for variable-cell relaxation calculations of P in the $A7$ structure with target pressures between 0 and 25 GPa.

A comparison can be made between the calculated frequency moments, $N(\epsilon_F)$, and λ for As in Ref. 23 and for P in the present work. We compare several quantities for sc As and P at pressures for which the calculated T_c is maximal for each material. For As at a calculated pressure of 30 GPa, $\lambda = 0.50$, $N(\epsilon_F) = 0.290$ states/eV atom, $\langle\omega^2\rangle^{1/2} = 284$ K, and $\omega_{\rm ln} = 253$ K. The corresponding quantities for P at 20 GPa are given in Table II. The atomic mass of P is 30.97, while that of As is 74.92. With reference to Eq. (10), the P to As ratios of the quantities λ, $N(\epsilon_F)$, $\langle g^2\rangle$, and $1/M\langle\omega^2\rangle$ are 1.59, 1.01, 1.63, and 0.97, respectively. Thus, the difference in λ between P and As at these specific pressures is mostly due to differences in $\langle g^2\rangle$. Additionally, the P to As ratio of $\omega_{\rm ln}$ is 1.65.

We can conclude that the larger $\omega_{\rm ln}$ and larger matrix elements contribute to a larger maximum T_c in P as compared with As. One should note that the $\mu^* \approx 0.12$ used in Ref. 23 is somewhat smaller than that needed in the present work ($\mu^* \approx 0.18$) to match T_c to experiment; the origin of this difference is unclear.

Comparing the trends as a function of pressure, both P and As in the sc structure have decreasing λ with increasing pressure, due mainly to the increase in phonon frequencies. Both elements have increasing $\langle g^2\rangle$ with increasing pressure in the sc structure.

B. Comparison to experiment: Structure, *e-p* coupling, and T_c

Our calculations can explain the decrease in T_c with increasing pressure above 30 GPa observed by Karuzawa *et al.*[18] in sc P as coming from the increase in phonon frequencies, which decreases λ. A similar physical effect occurs in As.[23] However, the decrease in T_c with decreasing pressure below 30 GPa remains unexplained by our calculations. Nor do our results indicate a constant T_c with pressure, as observed by Kawamura *et al.*,[15,16] nor any two-peak structure, as observed by Wittig *et al.*[17] In addition, our calculated $A7$ to sc transition pressure is significantly higher than what is found experimentally at room temperature. In this section, we suggest several possible explanations for the discrepancy between experiment and calculation which may serve as guide for future studies.

We consider the question of the structure of P as a function of pressure. Experimentally, the $A7$ to sc transition pressure is around 10 GPa at both room temperature[10,11] and higher temperatures,[67,68] and the pressure region of coexistence of the two phases is fairly narrow. At lower temperatures the transition pressure increases, and the region of coexistence broadens (12–15.5 GPa at 21 K).[69–71] Thus there is some experimental uncertainty about the actual lowest free-energy structure at a given pressure in this range at low temperature.

Our calculations determine whether $A7$ or sc has the lowest enthalpy structure at zero temperature at specified pressures. According to our calculations, the true $A7$ to sc transition, when α reaches 60° and u reaches 0.25, occurs at a calculated pressure above 15 GPa, corresponding to an experimental pressure of about 20–23 GPa (see Table I). Such a pressure is higher than any experimentally measured transition pressure.

Several possible explanations for the difference between calculation and experiment are presented here. First, our calculations do not include the zero-point energy (ZPE) or finite-temperature effects. If the fully anharmonic ZPE is included, the sc structure may in fact be stable below the calculated pressure of 15 GPa, and possibly down to a calculated pressure of 5 GPa, corresponding to about 13 GPa in experiment, for which our calculations show that α is still close to 60°. Such a scenario would resolve much of the discrepancy with experiment.

Another possibility is that an $A7$ structure, with α close to but not equal to 60°, and $u \neq 0.25$ actually remains stable

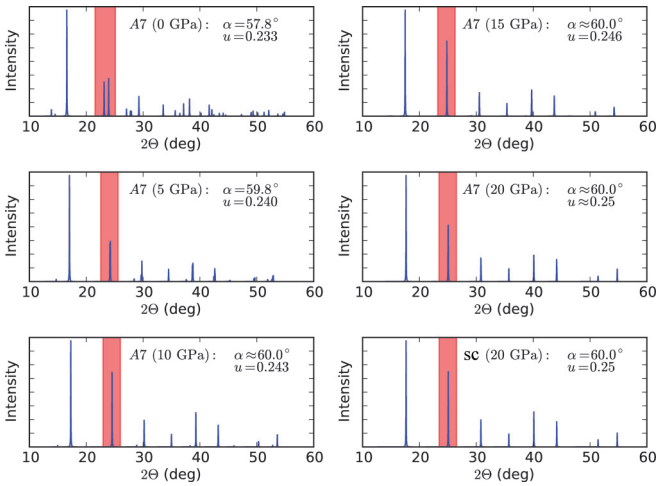

FIG. 9. (Color online) Simulated x-ray-diffraction spectra for relaxed $A7$ and sc structures at various pressures. The 10.4 and 11.0 (hkl) diffraction lines discussed in the text are highlighted for clarity. These lines appear to merge before the transition to the sc phase (with $u = 0.25$) is completed.

to pressures higher than what is quoted in the experimental works. Experimentally, the $A7$ to sc transition is determined by observation of the merging of diffraction lines 10.4 and 11.0 (hkl), which occur around $2\Theta \approx 24^\circ$, and the u parameter is not determined accurately.[11] We simulate x-ray-diffraction (XRD) spectra using the PLATON crystallographic tool[72] with Mo $K\alpha$ radiation and find that for our relaxed structures at 5–15 GPa, with α close to 60° and $u \neq 0.25$, the spectra look very close to spectra for the sc structure (Fig. 9). In particular, the merging of the 10.4 and 11.0 diffraction lines occurs already at 5 GPa (see highlighted region in Fig. 9), when the $A7$ structure is lower in energy and the u parameter is still relatively far from its cubic value of 0.25. Experimental broadening and background may make the two structures difficult to distinguish with this method.

It is also possible that use of the GGA or another functional for exchange and correlation, instead of the LDA, would give better agreement with experiment for the structure as a function of pressure. However, in the case of As, the $A7$ to sc transition pressure is *higher* for the GGA than for the LDA.[63] If the same holds true for P, then the GGA will be in further disagreement with experiment than the LDA. Experimental studies that determine u accurately as a function of pressure, and theoretical determination of the structure as a function of pressure, including ZPE and temperature effects and considering different functionals, would be useful in resolving this issue.

We now turn to the question of why, experimentally, T_c decreases with decreasing pressure below the peak. From a theoretical perspective, this question cannot be answered without first resolving the structure at these pressures. However, we can speculate based on the possible answers to the structural question.

If the structure is indeed sc down to an experimental pressure of ∼10 GPa, then the explanation of the T_c versus pressure trend may require going beyond the approximations made in the present study. It is possible that the full anharmonicity of the phonons must be considered, as was done for MgB_2.[5,73,74] As shown in the present study, anharmonicity raises the R phonon frequency significantly; if it raises the overall phonon frequencies throughout the BZ, it could reduce λ, leading to a lower T_c.[5] Multiple-phonon processes leading to nonlinear terms in the e-p coupling might also be important.[73,74] Also, inclusion of zero-point motion may have some effect on the electronic structure and $N(\epsilon_F)$, which could affect λ. It is also possible that one may need to go beyond the isotropic approximation to Eliashberg theory[75] assumed in the present work.

If the structure is in fact $A7$ at these pressures, then the decrease in T_c could be explained by a decrease in $N(\epsilon_F)$ as the $A7$ structure becomes more and more distorted from the sc one as pressure is lowered. A similar mechanism occurs for As and was elucidated in previous works.[23,55]

Finally, we note an interesting observation that the two structural transitions that we have found from our relaxation calculations, occurring between 0 and 5 GPa and 15 and 20 GPa, correspond well with the two T_c peaks at 12 and 23 GPa observed by Wittig *et al.*,[17] when the pressure shift due to the LDA is accounted for. It would be interesting to investigate whether this observation has physical significance.

V. CONCLUSION

In this study, we calculate the e-p coupling and T_c for phosphorus in the sc phase over the pressure range 20–70 GPa. Unlike prior theoretical results, our calculations explicitly treat the pressure dependence of the lattice dynamics. The decrease in T_c above 30 GPa is in good agreement with the experimental results of Karuzawa *et al.*[18] and can be explained as coming from the increase in phonon frequencies. The decrease in T_c as pressure is decreased below 30 GPa in sc P remains unexplained, but we suggest several possible routes to understanding this puzzle. Calculations of the $A7$ and sc structures in P reveal an interesting two-step transition which merits further study.

ACKNOWLEDGMENTS

This work was supported by National Science Foundation Grant No. DMR10-1006184 and by the Director, Office of Science, Office of Basic Energy Sciences, Materials Sciences and Engineering Division, U.S. Department of Energy under Contract No. DE-AC02-05CH11231. Computational support was provided by NSF through XSEDE resources at NICS and by DOE at Lawrence Berkeley National Laboratory's NERSC facility.

[1] H. Kamerlingh Onnes, Commun. Phys. Lab. Univ. Leiden **120b** (1911), reprinted in Proc. K. Ned. Akad. Wet. **13**, 1274 (1911).

[2] Y. Kamihara, T. Watanabe, M. Hirano, and H. Hosono, J. Am. Chem. Soc. **130**, 3296 (2008).

[3] K. Ishida, Y. Nakai, and H. Hosono, J. Phys. Soc. Jpn. **78**, 052001 (2009).

[4] J. Nagamatsu, N. Nakagawa, T. Muranaka, Y. Zenitani, and J. Akimitsu, Nature (London) **410**, 63 (2001).

[5]H. J. Choi, D. Roundy, H. Sun, M. L. Cohen, and S. G. Louie, Phys. Rev. B **66**, 020513 (2002).

[6]E. A. Ekimov, V. A. Sidorov, E. D. Bauer, N. N. Mel'nik, N. J. Curro, J. D. Thompson, and S. M. Stishov, Nature (London) **428**, 542 (2004).

[7]E. Bustarret, C. Marcenat, P. Achatz, J. Kačmarčik, F. Lévy, A. Huxley, L. Ortéga, E. Bourgeois, X. Blase, D. Débarre, and J. Boulmer, Nature (London) **444**, 465 (2006).

[8]K. Shimizu, H. Ishikawa, D. Takao, T. Yagi, and K. Amaya, Nature (London) **419**, 597 (2002).

[9]C. Buzea and K. Robbie, Supercond. Sci. Technol. **18**, R1 (2005).

[10]J. C. Jamieson, Science **139**, 1291 (1963).

[11]T. Kikegawa and H. Iwasaki, Acta Crystallogr. Sect. B: Struct. Sci. **39**, 158 (1983).

[12]Y. Akahama, M. Kobayashi, and H. Kawamura, Phys. Rev. B **59**, 8520 (1999).

[13]J. Wittig and B. T. Matthias, Science **160**, 994 (1968).

[14]I. V. Berman and N. B. Brandt, Pis'ma Zh. Eksp Teor. Fiz. **7**, 412 (1968) [JETP Lett. **7**, 326 (1968)].

[15]H. Kawamura, I. Shirotani, and K. Tachikawa, Solid State Commun. **49**, 879 (1984).

[16]H. Kawamura, I. Shirotani, and K. Tachikawa, Solid State Commun. **54**, 775 (1985).

[17]J. Wittig, B. Bireckoven, and T. Weidlich, in *Solid State Physics Under Pressure*, edited by S. Minomura (KTK Scientific, Tokyo, 1985), p. 127.

[18]M. Karuzawa, M. Ishizuka, and S. Endo, J. Phys.: Condens. Matter **14**, 10759 (2002).

[19]M. Rajagopalan, M. Alouani, and N. E. Christensen, J. Low Temp. Phys. **75**, 1 (1989).

[20]M. Aoki, N. Suzuki, and K. Motizuki, J. Phys. Soc. Jpn. **56**, 3253 (1987).

[21]H. Nagara, K. Mukose, T. Ishikawa, M. Geshi, and N. Suzuki, J. Phys.: Conf. Series **215**, 012107 (2010).

[22]L. W. Nixon, Ph.D. thesis, George Mason University, 2010.

[23]K. T. Chan, B. D. Malone, and M. L. Cohen, Phys. Rev. B **86**, 094515 (2012).

[24]P. B. Allen, Phys. Rev. B **6**, 2577 (1972).

[25]W. L. McMillan, Phys. Rev. **167**, 331 (1968).

[26]P. B. Allen and R. C. Dynes, Phys. Rev. B **12**, 905 (1975).

[27]P. Morel and P. W. Anderson, Phys. Rev. **125**, 1263 (1962).

[28]P. Giannozzi, S. Baroni, N. Bonini, M. Calandra, R. Car, C. Cavazzoni, D. Ceresoli, G. L. Chiarotti, M. Cococcioni, I. Dabo, A. Dal Corso, S. de Gironcoli, S. Fabris, G. Fratesi, R. Gebauer, U. Gerstmann, C. Gougoussis, A. Kokalj, M. Lazzeri, L. Martin-Samos, N. Marzari, F. Mauri, R. Mazzarello, S. Paolini, A. Pasquarello, L. Paulatto, C. Sbraccia, S. Scandolo, G. Sclauzero, A. P. Seitsonen, A. Smogunov, P. Umari, and R. M. Wentzcovitch, J. Phys.: Condens. Matter **21**, 395502 (2009).

[29]P. Hohenberg and W. Kohn, Phys. Rev. **136**, B864 (1964).

[30]W. Kohn and L. J. Sham, Phys. Rev. **140**, A1133 (1965).

[31]J. Ihm, A. Zunger, and M. L. Cohen, J. Phys. C **12**, 4409 (1979).

[32]M. L. Cohen, Phys. Scr. **T1**, 5 (1982).

[33]D. M. Ceperley and B. J. Alder, Phys. Rev. Lett. **45**, 566 (1980).

[34]J. P. Perdew and A. Zunger, Phys. Rev. B **23**, 5048 (1981).

[35]N. Troullier and J. L. Martins, Phys. Rev. B **43**, 1993 (1991).

[36]M. J. T. Oliveira and F. Nogueira, Comput. Phys. Commun. **178**, 524 (2008).

[37]S. G. Louie, S. Froyen, and M. L. Cohen, Phys. Rev. B **26**, 1738 (1982).

[38]H. J. Monkhorst and J. D. Pack, Phys. Rev. B **13**, 5188 (1976).

[39]N. Marzari, D. Vanderbilt, A. De Vita, and M. C. Payne, Phys. Rev. Lett. **82**, 3296 (1999).

[40]F. Giustino, M. L. Cohen, and S. G. Louie, Phys. Rev. B **76**, 165108 (2007).

[41]J. Noffsinger, F. Giustino, B. D. Malone, C.-H. Park, S. G. Louie, and M. L. Cohen, Comput. Phys. Commun. **181**, 2140 (2010).

[42]N. Marzari and D. Vanderbilt, Phys. Rev. B **56**, 12847 (1997).

[43]I. Souza, N. Marzari, and D. Vanderbilt, Phys. Rev. B **65**, 035109 (2001).

[44]A. A. Mostofi, J. R. Yates, Y.-S. Lee, I. Souza, D. Vanderbilt, and N. Marzari, Comput. Phys. Commun. **178**, 685 (2008).

[45]S. Baroni, S. de Gironcoli, A. Dal Corso, and P. Giannozzi, Rev. Mod. Phys. **73**, 515 (2001).

[46]F. Birch, Phys. Rev. **71**, 809 (1947).

[47]T. Sasaki, K. Shindo, K. Niizeki, and A. Morita, J. Phys. Soc. Jpn. **57**, 978 (1988).

[48]A. Nishikawa, K. Niizeki, and K. Shindo, Phys. Status Solidi B **223**, 189 (2001).

[49]R. Ahuja, Phys. Status Solidi B **235**, 282 (2003).

[50]D. Kasinathan, J. Kuneš, A. Lazicki, H. Rosner, C. S. Yoo, R. T. Scalettar, and W. E. Pickett, Phys. Rev. Lett. **96**, 047004 (2006).

[51]G. Profeta, C. Franchini, N. N. Lathiotakis, A. Floris, A. Sanna, M. A. L. Marques, M. Lüders, S. Massidda, E. K. U. Gross, and A. Continenza, Phys. Rev. Lett. **96**, 047003 (2006).

[52]T. Bazhirov, J. Noffsinger, and M. L. Cohen, Phys. Rev. B **82**, 184509 (2010).

[53]T. Bazhirov, J. Noffsinger, and M. L. Cohen, Phys. Rev. B **84**, 125122 (2011).

[54]A. S. Mikhaylushkin, S. I. Simak, B. Johansson, and U. Häussermann, Phys. Rev. B **76**, 092103 (2007).

[55]A. L. Chen, S. P. Lewis, Z. Su, P. Y. Yu, and M. L. Cohen, Phys. Rev. B **46**, 5523 (1992).

[56]K. H. Bennemann and J. W. Garland, *Superconductivity in d- and f- Band Metals,* edited by H. C. Wolfe and D. H. Douglass, AIP Conf. Proc. No. 4 (AIP, New York, 1972), p. 103.

[57]J. W. Garland and K. H. Bennemann, *Superconductivity in d- and f- Band Metals,* AIP Conf. Proc. No. 4 (Ref. 56), p. 255.

[58]D. Papaconstantopoulos and B. Klein, Physica B + C **107**, 725 (1981).

[59]C. F. Richardson and N. W. Ashcroft, Phys. Rev. B **55**, 15130 (1997).

[60]C. R. da Silva and R. M. Wentzcovitch, Comput. Mater. Sci. **8**, 219 (1997).

[61]M. Durandurdu, Phys. Rev. B **72**, 073208 (2005).

[62]W. Feng, S. Cui, H. Hu, and H. Liu, Physica B: Condens. Matter **400**, 22 (2007).

[63]P. Silas, J. R. Yates, and P. D. Haynes, Phys. Rev. B **78**, 174101 (2008).

[64]T. Kikegawa and H. Iwasaki, J. Phys. Soc. Jpn. **56**, 3417 (1987).

[65]H. J. Beister, K. Strössner, and K. Syassen, Phys. Rev. B **41**, 5535 (1990).

[66]S. Shang, Y. Wang, H. Zhang, and Z.-K. Liu, Phys. Rev. B **76**, 052301 (2007).

[67]H. Iwasaki, T. Kikegawa, T. Fujimura, S. Endo, Y. Akahama, T. Akai, O. Shimomura, S. Yamaoka, T. Yagi, S. Akimoto, and I. Shirotani, Physica B + C **139–140**, 301 (1986).

[68]T. Kikegawa, H. Iwasaki, T. Fujimura, S. Endo, Y. Akahama, T. Akai, O. Shimomura, T. Yagi, S. Akimoto, and I. Shirotani, J. Appl. Crystallogr. **20**, 406 (1987).
[69]I. Shirotani, H. Kawamura, K. Tsuji, K. Tsuburaya, O. Shimomura, and K. Tachikawa, Bull. Chem. Soc. Jpn. **61**, 211 (1988).
[70]I. Shirotani, K. Tsuji, M. Imai, H. Kawamura, O. Shimomura, T. Kikegawa, and T. Nakajima, Phys. Lett. A **144**, 102 (1990).
[71]I. Shirotani, J. Mikami, T. Adachi, Y. Katayama, K. Tsuji, H. Kawamura, O. Shimomura, and T. Nakajima, Phys. Rev. B **50**, 16274 (1994).
[72]A. L. Spek, Acta Crystallogr. Sec. D **65**, 148 (2009).
[73]T. Yildirim, O. Gülseren, J. W. Lynn, C. M. Brown, T. J. Udovic, Q. Huang, N. Rogado, K. A. Regan, M. A. Hayward, J. S. Slusky, T. He, M. K. Haas, P. Khalifah, K. Inumaru, and R. J. Cava, Phys. Rev. Lett. **87**, 037001 (2001).
[74]A. Y. Liu, I. I. Mazin, and J. Kortus, Phys. Rev. Lett. **87**, 087005 (2001).
[75]P. B. Allen and B. Mitrović, in *Solid State Physics*, edited by H. Ehrenreich, F. Seitz, and D. Turnbull (Academic, New York, 1983), Vol. 37, pp. 1–92.